frontiers in Physics

MINI REVIEW
published: 22 February 2021
doi: 10.3389/fphy.2021.599146

Instability of Double-Periodic Waves in the Nonlinear Schrödinger Equation

Dmitry E. Pelinovsky*

Department of Mathematics, McMaster University, Hamilton, ON, Canada

It is shown how to compute the instability rates for the double-periodic solutions to the cubic NLS (nonlinear Schrödinger) equation by using the Lax linear equations. The wave function modulus of the double-periodic solutions is periodic both in space and time coordinates; such solutions generalize the standing waves which have the time-independent and space-periodic wave function modulus. Similar to other waves in the NLS equation, the double-periodic solutions are spectrally unstable and this instability is related to the bands of the Lax spectrum outside the imaginary axis. A simple numerical method is used to compute the unstable spectrum and to compare the instability rates of the double-periodic solutions with those of the standing periodic waves.

Keywords: modulational instability, double-periodic solutions, Floquet spectrum, nonlinear Schrödinger equation, standing waves

OPEN ACCESS

Edited by:
Heremba Bailung,
Ministry of Science and Technology, India

Reviewed by:
Maximo Aguero,
Universidad Autónoma del Estado de México, Mexico
Constance Schober,
University of Central Florida, United States

Correspondence:
Dmitry E. Pelinovsky
dmpeli@math.mcmaster.ca

Specialty section:
This article was submitted to Mathematical and Statistical Physics, a section of the journal Frontiers in Physics

Received: *26 August 2020*
Accepted: *04 January 2021*
Published: *22 February 2021*

Citation:
Pelinovsky DE (2021) Instability of Double-Periodic Waves in the Nonlinear Schrödinger Equation. Front. Phys. 9:599146. doi: 10.3389/fphy.2021.599146

1 INTRODUCTION

Peregrine breather is a rogue wave arising on the background of the constant-amplitude wave due to its modulational instability [1, 2]. The focusing cubic NLS (nonlinear Schrödinger) equation is the canonical model which describes both the modulational instability and the formation of rogue waves. Formation of rogue waves on the constant-amplitude background have been modeled from different initial data such as local condensates [3], multi-soliton gases [4–6], and periodic perturbations [7, 8]. Rogue waves have been experimentally observed both in hydrodynamical and optical laboratories [9] (see recent reviews in [10, 11]).

Mathematical theory of rogue waves on the constant-amplitude background has seen many recent developments. universal behavior of the modulationally unstable constant-amplitude background was studied asymptotically in [12, 13]. The finite-gap method was employed to relate the unstable modes on the constant-amplitude background with the occurrence of rogue waves [14, 15]. Rogue waves of infinite order were constructed in [16] based on recent developments in the inverse scattering method [17]. Rogue waves of the soliton superposition were studied asymptotically in the limit of many solitons [18, 19].

At the same time, rogue waves were also investigated on the background of standing periodic waves expressed by the Jacobian elliptic functions. Such exact solutions to the NLS equation were constructed first in [20] (see also early numerical work in [21] and the recent generalization in [22]). It was confirmed in [23] that these rogue waves arise due to the modulational instability of the standing periodic waves [24] (see also [25, 26]). Instability of the periodic standing waves can be characterized by the separation of variables in the Lax system of linear equations [27] (see also [28, 29]), compatibility of which gives the NLS equation. Instability and rogue waves on the background of standing periodic waves have been experimentally observed in [30].

The main goal of this paper is to compute the instability rates for the double-periodic solutions to the NLS equation, for which the wave function modulus is periodic with respect to both space and time coordinates. In particular, we consider two families of double-periodic solutions expressed as rational functions of the Jacobian elliptic functions which were constructed in the pioneering work [31]. These solutions represent perturbations of the Akhmediev breathers and describe generation of either phase-repeated or phase-alternating wave patterns [32, 33]. Rogue waves on the background of the double-periodic solutions were studied in [34] (see also numerical work in [35, 36]). Experimental observation of the double-periodic solutions in optical fibers was reported in [37].

The double-periodic solutions constructed in [31] are particular cases of the quasi-periodic solutions of the NLS equation given by the Riemann Theta functions of genus two [38–40]. Rogue waves for general quasi-periodic solutions of any genus were considered in [41–43].

Instability of the double-periodic solutions is studied using the Floquet theory for the Lax system of linear equations both in space and time coordinates. We compute the instability rates of the double-periodic solutions and compare them with those for the standing periodic waves. In order to provide a fair comparison, we normalize the amplitude of all solutions to unity. *As a main outcome of this work, we show that the instability rates are larger for the constant-amplitude waves and smaller for the double-periodic waves.*

The article is organized as follows. The explicit solutions to the NLS equation are reviewed in **Section 2**. Instability rates for the standing periodic waves and the double-periodic solutions are computed in **Sections 3 and 4** respectively. Further directions are discussed in **Section 5**.

2 EXPLICIT SOLUTIONS TO THE NLS EQUATION

The nonlinear Schrödinger (NLS) equation is a fundamental model for nonlinear wave dynamics [44, 45]. We take the NLS equation in the standard form:

$$i\psi_t + \frac{1}{2}\psi_{xx} + |\psi|^2\psi = 0. \tag{2.1}$$

This model has several physical symmetries which are checked directly:

- translation:

$$\text{if } \psi(x,t) \text{ is a solution, so is } \psi(x+x_0, t+t_0), \text{ for every } (x_0,t_0) \in \mathbb{R}\times\mathbb{R}, \tag{2.2}$$

- scaling:

$$\text{if } \psi(x,t) \text{ is a solution, so is } \alpha\psi(\alpha x, \alpha^2 t), \text{ for every } \alpha \in \mathbb{R}, \tag{2.3}$$

- Lorentz transformation:

$$\text{if } \psi(x,t) \text{ is a solution, so is } \psi(x+\beta t, t)e^{-i\beta x - \frac{i}{2}\beta^2 t}, \text{ for every } \beta \in \mathbb{R}. \tag{2.4}$$

In what follows, we use the scaling symmetry **Eq. 2.3** to normalize the amplitude of periodic and double-periodic solutions to unity and the Lorentz symmetry **Eq. 2.4** to set the wave speed to zero. We also neglect the translational parameters (x_0, t_0) due to the symmetry **Eq. 2.2**.

A solution $\psi(x,t) : \mathbb{R}\times\mathbb{R} \to \mathbb{C}$ to the NLS **Eq. 2.1** is a compatibility condition of the Lax system of linear equations on $\varphi(x,t) : \mathbb{R}\times\mathbb{R} \to \mathbb{C}^2$:

$$\varphi_x = U(\lambda,\psi)\varphi, \; U(\lambda,\psi) = \begin{pmatrix} \lambda & \psi \\ -\overline{\psi} & -\lambda \end{pmatrix} \tag{2.5}$$

and

$$\varphi_t = V(\lambda,\psi)\varphi, V(\lambda,\psi) = i\begin{pmatrix} \lambda^2 + \frac{1}{2}|\psi|^2 & \frac{1}{2}\psi_x + \lambda\psi \\ \frac{1}{2}\overline{\psi}_x - \lambda\overline{\psi} & -\lambda^2 - \frac{1}{2}|\psi|^2 \end{pmatrix}, \tag{2.6}$$

where $\overline{\psi}$ is the conjugate of ψ and $\lambda \in \mathbb{C}$ is a spectral parameter.

The algebraic method developed in [34] allows us to construct the stationary (Lax–Novikov) equations which admit a large class of bounded periodic and quasi-periodic solutions to the NLS **Eq. 2.1**. The simplest first-order Lax–Novikov equation is given by

$$\frac{du}{dx} + 2icu = 0, \tag{2.7}$$

where c is arbitrary real parameter. A general solution of this equation is given by $u(x) = Ae^{-2icx}$, where A is the integration constant. This solution determines the constant-amplitude waves of the NLS **Eq. 2.1** in the form:

$$\psi(x,t) = Ae^{-2ic(x+ct)+iA^2 t}, \tag{2.8}$$

where $A > 0$ is the constant amplitude and translations in (x,t) are neglected due to the translational symmetry **Eq. 2.2**. Without loss of generality, c can be set to 0 due to the Lorentz transformation. Indeed, transformation **Eq. 2.4** with $\beta = -c$ transforms **Eq. 2.8** to the equivalent form $\psi(x,t) = Ae^{-icx-\frac{i}{2}c^2 t + iA^2 t}$, which is obtained from $\psi(x,t) = Ae^{-iA^2 t}$ due to transformation **Eq. 2.4** with $\beta = c$. By the scaling transformation **Eq. 2.3** with $\alpha = A^{-1}$, the amplitude A can be set to unity, which yields the normalized solution $\psi(x,t) = e^{it}$.

The second-order Lax–Novikov equation is given by

$$\frac{d^2u}{dx^2} + 2|u|^2 u + 2ic\frac{du}{dx} - 4bu = 0, \tag{2.9}$$

where (c,b) are arbitrary real parameters. Solutions u to the second-order **Eq. 2.9** determines the standing traveling waves of the NLS **Eq. 2.1** in the form:

$$\psi(x,t) = u(x+ct)e^{2ibt}. \tag{2.10}$$

Without loss of generality, we set $c = 0$ due to the Lorentz transformation **Eq. 2.4** with $\beta = -c$. Waves with the trivial phase are of particular interest [20, 27]. There are two families of such standing periodic waves given by the Jacobian elliptic functions in the form:

$$\psi(x,t) = \mathrm{dn}(x;k)e^{i\left(1-k^2/2\right)t} \tag{2.11}$$

and

$$\psi(x,t) = k\mathrm{cn}(x;k)e^{i\left(k^2-1/2\right)t}, \tag{2.12}$$

where the parameter $k \in (0,1)$ is the elliptic modulus. The solutions **Eqs. 2.11, 2.12** are defined up to the scaling transformation **Eq. 2.3** and translations **Eq. 2.2**. The amplitude (maximal value of $|\psi|$) is set to unity for **Eq. 2.11** and to k for **Eq. 2.12**. In order to normalize the amplitude to unity for the cnoidal wave **Eq. 2.12**, we can use the scaling transformation **Eq. 2.3** with $\alpha = k^{-1}$.

Due to the well-known expansion formulas

$$\begin{aligned}
\mathrm{dn}(x;k) &= \mathrm{sech}(x) + \frac{1}{4}\left(1-k^2\right)\left[\sinh(x)\cosh(x)+x\right] \\
&\quad \times \tanh(x)\mathrm{sech}(x) + \mathcal{O}\left(\left(1-k^2\right)^2\right), \\
\mathrm{cn}(x;k) &= \mathrm{sech}(x) - \frac{1}{4}\left(1-k^2\right)\left[\sinh(x)\cosh(x)-x\right] \\
&\quad \times \tanh(x)\mathrm{sech}(x) + \mathcal{O}\left(\left(1-k^2\right)^2\right),
\end{aligned}$$

both the periodic waves **Eqs. 2.11, 2.12** approaches the NLS soliton $\psi(x,t) = \mathrm{sech}(x)e^{it/2}$ as $k \to 1$. In the other limit, the dnoidal periodic wave **Eq. 2.11** approaches the constant-amplitude wave $\psi(x,t) = e^{it}$ as $k \to 0$, whereas the normalized cnoidal periodic wave **Eq. 2.12** approaches the harmonic wave $\psi(x,t) \sim \cos(x/k)e^{-it/(2k^2)}$ as $k \to 0$.

The third-order Lax–Novikov equation is given by

$$\frac{d^3u}{dx^3} + 6|u|^2\frac{du}{dx} + 2ic\left(\frac{d^2u}{dx^2} + 2|u|^2u\right) - 4b\frac{du}{dx} + 8iau = 0, \tag{2.13}$$

where (a,b,c) are arbitrary real parameters. Waves with $a = c = 0$ are again of particular interest [31]. After a transformation of variables [34], such solutions can be written in the form:

$$\psi(x,t) = \left[Q(x,t) + i\delta(t)\right]e^{i\theta(t)}, \tag{2.14}$$

where $Q(x,t): \mathbb{R}\times\mathbb{R} \to \mathbb{R}$ is periodic both in the space and time coordinates and $\delta(t): \mathbb{R} \to \mathbb{R}$ has a double period in t compared to $Q(x,t)$. There are two particular families of the double-periodic solutions **Eq. 2.14**, which can be written by using the Jacobian elliptic functions (see Appendices A and B in [34]):

$$\begin{aligned}
\psi(x,t) &= k\frac{\mathrm{cn}(t;k)\mathrm{cn}\left(\sqrt{1+k}\,x;\kappa\right) + i\sqrt{1+k}\,\mathrm{sn}(t;k)\mathrm{dn}\left(\sqrt{1+k}\,x;\kappa\right)}{\sqrt{1+k}\,\mathrm{dn}\left(\sqrt{1+k}\,x;\kappa\right) - \mathrm{dn}(t;k)\mathrm{cn}\left(\sqrt{1+k}\,x;\kappa\right)}e^{it}, \\
\kappa &= \frac{\sqrt{1-k}}{\sqrt{1+k}}
\end{aligned} \tag{2.15}$$

and

$$\begin{aligned}
\psi(x,t) &= \frac{\mathrm{dn}(t;k)\mathrm{cn}\left(\sqrt{2}\,x;\kappa\right) + i\sqrt{k(1+k)}\,\mathrm{sn}(t;k)}{\sqrt{1+k} - \sqrt{k}\,\mathrm{cn}(t;k)\mathrm{cn}\left(\sqrt{2}\,x;\kappa\right)}e^{ikt}, \\
\kappa &= \frac{\sqrt{1-k}}{\sqrt{2}},
\end{aligned} \tag{2.16}$$

where $k \in (0,1)$ is the elliptic modulus. The solutions **Eqs. 2.15, 2.16** are defined up to the scaling transformation **Eq. 2.3** and the translations **Eq. 2.2**. The amplitude (maximal value of $|u|$) is $\sqrt{1+k}+1$ for **Eq. 2.15** and $\sqrt{1+k}+\sqrt{k}$ for **Eq. 2.16**. In order to normalize the amplitudes of the double-periodic waves to unity, we can use the scaling transformation **Eq. 2.3** with $\alpha = \left(\sqrt{1+k}+1\right)^{-1}$ and $\alpha = \left(\sqrt{1+k}+\sqrt{k}\right)^{-1}$ respectively.

The double-periodic solutions **Eqs. 2.15, 2.16** can be written in the form:

$$\psi(x,t) = \phi(x,t)e^{2ibt}, \quad \phi(x+L,t) = \phi(x,t+T) = \phi(x,t), \tag{2.17}$$

where $L > 0$ and $T > 0$ are fundamental periods in space and time coordinates, respectively, whereas $2b = 1$ for **Eq. 2.15** and $2b = k$ for **Eq. 2.16**.

Figure 1 shows surface plots of $|\psi|$ on the (x,t) plane within the fundamental periods. The amplitudes of the double-periodic waves on **Figure 1** have been normalized to unity by the scaling transformation **Eq. 2.3**. The solution **Eq. 2.15** generates the phase-repeated wave patterns, whereas the solution **Eq. 2.16** generates the phase-alternating patterns [32–34, 36].

As $k \to 1$, both the double-periodic solutions **Eqs. 2.15** and **2.16** approach to the same Akhmediev breather given by

$$\psi(x,t) = \frac{\cos\left(\sqrt{2}\,x\right) + i\sqrt{2}\sinh(t)}{\sqrt{2}\cosh(t) - \cos\left(\sqrt{2}\,t\right)}e^{it}. \tag{2.18}$$

As $k \to 0$, the solution **Eq. 2.15** approaches the scaled NLS soliton

$$\psi(x,t) = 2\mathrm{sech}(2x)e^{2it}, \tag{2.19}$$

whereas the solution **Eq. 2.16** approaches the scaled cnoidal wave

$$\psi(x,t) = \mathrm{cn}\left(\sqrt{2}\,x;\frac{1}{\sqrt{2}}\right). \tag{2.20}$$

These limits are useful to control accuracy of numerical computations of the modulational instability rate for the double-periodic solutions in comparison with the similar numerical computations for the standing waves.

3 INSTABILITY OF STANDING WAVES

Here we review how to use the linear **Eq. 2.5, 2.6** in order to compute the instability rates for the standing periodic waves (**Eq. 2.10**) (see [23, 27]). Due to the separation of variables in **Eq. 2.10**, one can write

$$\varphi_1(x,t) = \chi_1(x+ct)e^{ibt+t\Omega}, \quad \varphi_2(x,t) = \chi_2(x+ct)e^{-ibt+t\Omega}, \tag{3.1}$$

where $\Omega \in \mathbb{C}$ is another spectral parameter and $\chi = (\chi_1,\chi_2)^T$ satisfies the following spectral problems:

$$\chi_x = \begin{pmatrix} \lambda & u \\ -\bar{u} & -\lambda \end{pmatrix}\chi, \tag{3.2}$$

and

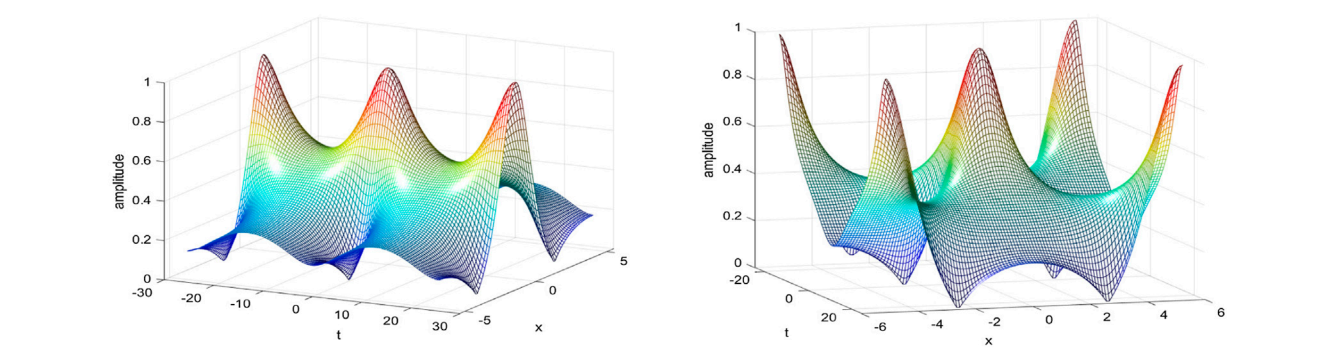

FIGURE 1 | Amplitude-normalized double-periodic waves **Eq. 2.15 (left)** and **Eq. 2.16 (right)** with $k = 0.9$.

$$\Omega\chi + c\begin{pmatrix} \lambda & u \\ -\bar{u} & -\lambda \end{pmatrix}\chi = i\begin{pmatrix} \lambda^2 + \frac{1}{2}|u|^2 - b & \frac{1}{2}\frac{du}{dx} + \lambda u \\ \frac{1}{2}\frac{d\bar{u}}{dx} - \lambda\bar{u} & -\lambda^2 - \frac{1}{2}|u|^2 + b \end{pmatrix}\chi. \tag{3.3}$$

We say that λ belongs to *the Lax spectrum* of the spectral problem **Eq. 3.2** if $\chi \in L^\infty(\mathbb{R})$. Since $u(x+L) = u(x)$ is periodic with the fundamental period $L > 0$, Floquet's Theorem guarantees that bounded solutions of the linear **Eq. 3.2** can be represented in the form:

$$\chi(x) = \hat{\chi}(x)e^{i\theta x}, \tag{3.4}$$

where $\hat{\chi}(x+L) = \hat{\chi}(x)$ and $\theta \in \left[-\frac{\pi}{L}, \frac{\pi}{L}\right]$. When $\theta = 0$ and $\theta = \pm\frac{\pi}{L}$, the bounded solutions **Eq. 3.4** are periodic and anti-periodic, respectively.

Since the spectral problem **Eq. (3.3)** is a linear algebraic system, it admits a nonzero solution if and only if the determinant of the coefficient matrix is zero. The latter condition yields the x-independent relation between Ω and λ in the form $\Omega^2 + P(\lambda) = 0$, where $P(\lambda)$ is given by

$$P(\lambda) = \lambda^4 + 2ic\lambda^3 - (c^2 + 2b)\lambda^2 + 2i(a - bc)\lambda + b^2 - 2ac + 2d, \tag{3.5}$$

with parameters a and d being the conserved quantities of the second-order **Eq. 2.9**:

$$\left|\frac{du}{dx}\right|^2 + |u|^4 - 4b|u|^2 = 8d, \tag{3.6}$$

and

$$i\left(\frac{du}{dx}\bar{u} - u\frac{d\bar{u}}{dx}\right) - 2c|u|^2 = 4a. \tag{3.7}$$

Polynomial $P(\lambda)$ naturally occurs in the algebraic method [34]. For the standing waves of the trivial phase with $a = c = 0$, the polynomial $P(\lambda)$ can be written explicitly in the form:

$$P(\lambda) = \lambda^4 - \frac{1}{2}(u_1^2 + u_2^2)\lambda^2 + \frac{1}{16}(u_1^2 - u_2^2)^2, \tag{3.8}$$

where the turning points u_1 and u_2 parameterize b and d in the form:

$$\begin{cases} 4b = u_1^2 + u_2^2, \\ 8d = -u_1^2u_2^2. \end{cases} \tag{3.9}$$

Roots of $P(\lambda)$ are located at $\{\pm\lambda_1, \pm\lambda_2\}$ given by

$$\lambda_1 = \frac{u_1 + u_2}{2}, \quad \lambda_2 = \frac{u_1 - u_2}{2}, \tag{3.10}$$

so that the polynomial $P(\lambda)$ can be written in the factorized form:

$$P(\lambda) = (\lambda^2 - \lambda_1^2)(\lambda^2 - \lambda_2^2). \tag{3.11}$$

By adding a perturbation v to the standing wave u in the form

$$\psi(x,t) = e^{2ibt}[u(x+ct) + v(x+ct,t)] \tag{3.12}$$

and dropping the quadratic terms in v, we obtain the linearized system of equations which describe linear stability of the standing waves (**Eq. 2.10**):

$$\begin{cases} iv_t - 2bv + icv_x + \frac{1}{2}v_{xx} + 2|u|^2v + u^2\bar{v} = 0, \\ -i\bar{v}_t - 2b\bar{v} - ic\bar{v}_x + \frac{1}{2}\bar{v}_{xx} + 2|u|^2\bar{v} + \bar{u}^2v = 0. \end{cases} \tag{3.13}$$

The variables can be separated in the form:

$$v(x,t) = w_1(x)e^{t\Lambda}, \quad \bar{v}(x,t) = w_2(x)e^{t\Lambda}, \tag{3.14}$$

where Λ is a spectral parameter and $w = (w_1, w_2)^T$ satisfies the spectral stability problem

$$i\Lambda\sigma_3 w + \begin{pmatrix} \frac{1}{2}\partial_x^2 + 2|u|^2 - 2b + ic\partial_x & u^2 \\ \bar{u}^2 & \frac{1}{2}\partial_x^2 + 2|u|^2 - 2b - ic\partial_x \end{pmatrix}w = 0, \tag{3.15}$$

where $\sigma_3 = \mathrm{diag}(1,-1)$. Note that w_1 and w_2 are no longer complex conjugate if $\Lambda \notin \mathbb{R}$.

We say that Λ belongs to *the stability spectrum* of the spectral problem **Eq. 3.15** if $w \in L^\infty(\mathbb{R})$. If λ is in the Lax spectrum of the spectral problem **Eq. 3.2**, then the bounded squared eigenfunctions χ_1^2 and χ_2^2 determine the bounded eigen

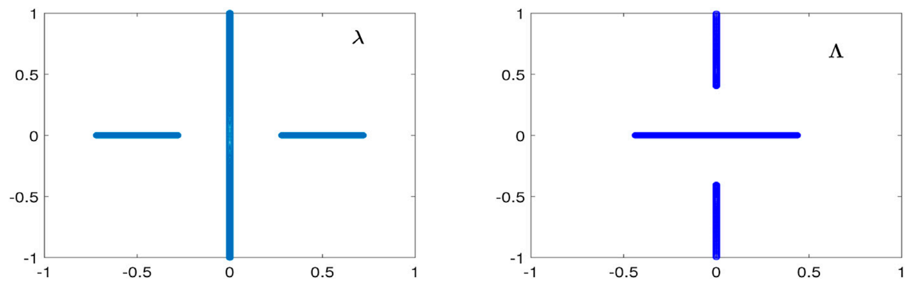

FIGURE 2 | Lax spectrum on the λ-plane **(left)** and stability spectrum on the Λ-plane **(right)** for the dn-periodic wave **Eq. 2.11** with $k = 0.9$.

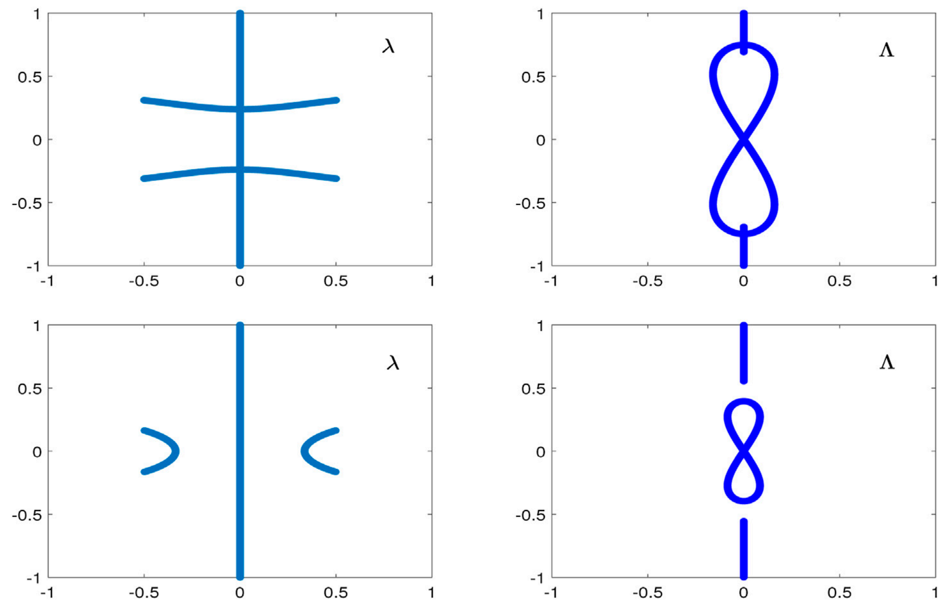

FIGURE 3 | The same as **Figure 2** but for the amplitude-normalized cn-periodic wave with $k = 0.85$ **(top)** and $k = 0.95$ **(bottom)**.

functions w_1 and w_2 of the spectral stability problem **Eq. 3.15** and Ω determines eigenvalues Λ as follows:

$$w_1 = \chi_1^2, \quad w_2 = -\chi_2^2, \quad \Lambda = 2\Omega. \tag{3.16}$$

Validity of **Eq. 3.16** can be checked directly from **Eqs. 3.2**, **3.3**, **3.14**, and **3.15**. If $\mathrm{Re}(\Lambda) > 0$ for λ in the Lax spectrum, the periodic standing wave **Eq. 2.10** is called *spectrally unstable*. It is called *modulationally unstable* if the unstable spectrum with $\mathrm{Re}(\Lambda) > 0$ intersects the origin in the Λ-plane transversely to the imaginary axis.

The importance of distinguishing between spectral and modulational instability of the periodic standing waves appears in the existence of rogue waves on their background. It was shown in [46] that if the periodic standing waves are spectrally unstable but modulationally stable, the rogue waves are not fully localized and degenerate into propagating algebraic solitons. Similarly, it was shown in [23] that if the unstable spectrum with $\mathrm{Re}(\Lambda) > 0$ intersects the origin in the Λ-plane tangentially to the imaginary axis, the corresponding rogue wave degenerates into a propagating algebraic soliton.

Next, we compute the instability rates for the standing periodic waves (2.10) of the trivial phase with $a = c = 0$. It follows from **Eq. 3.11** with either real λ_1, λ_2 or complex-conjugate $\lambda_1 = \bar{\lambda}_2$ that if $\lambda \in i\mathbb{R}$ belongs to the Lax spectrum, then $\Lambda \in i\mathbb{R}$ belongs to the stable spectrum. Thus, the spectral instability of the standing periodic waves of the trivial phase is only related to the Lax spectrum with $\lambda \notin i\mathbb{R}$.

For the dn-periodic wave **Eq. 2.11** with $u_1 = 1$ and $u_2 = \sqrt{1-k^2}$, the amplitude is already normalized to unity and no scaling transformation is needed. Lax spectrum of the spectral problem **Eq. 3.2** is shown on **Figure 2** (left) for $k = 0.9$. It follows from **Eq. 3.11** that $P(\lambda) < 0$ for $\lambda \in (\lambda_2, \lambda_1)$ with $P(\lambda_{1,2}) = 0$, where $\lambda_{1,2}$ are given by **Eq. 3.10**. The unstable spectrum on the Λ-plane belongs to the finite segment on the real line which touches the origin as is shown on **Figure 2** (right), hence the dn-periodic wave Eq. (2.11) is both spectrally and modulationally unstable. It follows from **Eq. 3.16** that

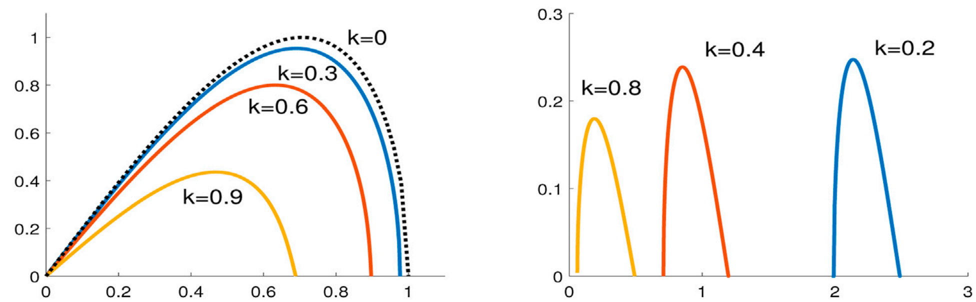

FIGURE 4 | Instability rate $\mathrm{Re}(\Lambda)$ versus the Floquet parameter θ for the amplitude-normalized dn-periodic **(left)** and cn-periodic **(right)** waves. The values of k in the elliptic functions are given in the plots.

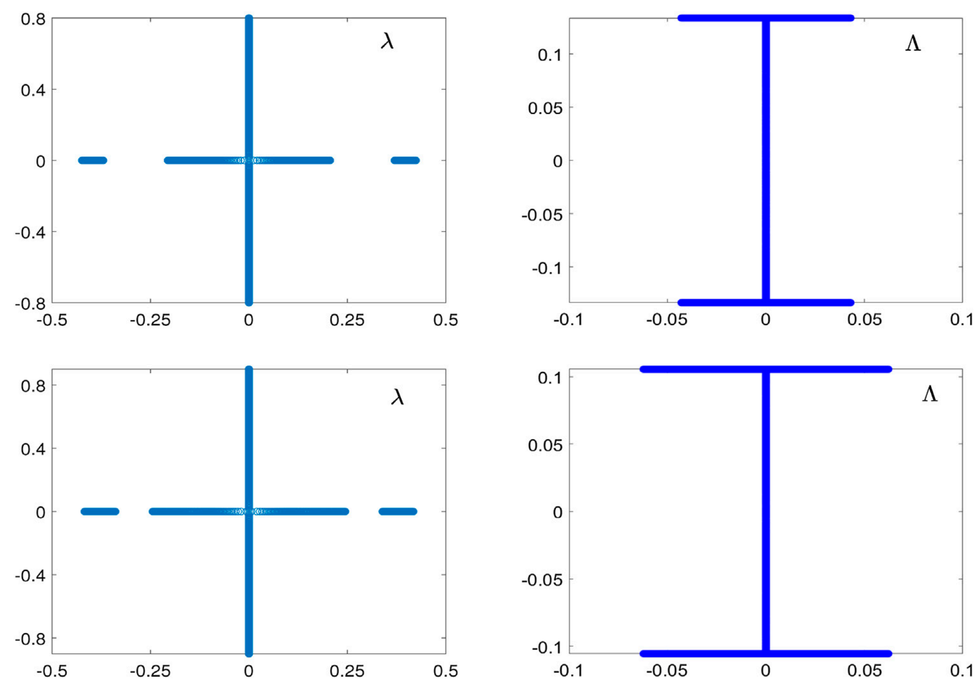

FIGURE 5 | Lax spectrum on the λ-plane **(left)** and stability spectrum on the Λ-plane **(right)** for the amplitude-normalized double-periodic wave **Eq. 2.15** with $k = 0.85$ **(top)** and $k = 0.95$ **(bottom)**.

$$\max_{\lambda \in [\lambda_2,\lambda_1]} \Lambda = \max_{\lambda \in [\lambda_2,\lambda_1]} 2\sqrt{(\lambda_1^2 - \lambda^2)(\lambda^2 - \lambda_2^2)} = (\lambda_1^2 - \lambda_2^2) = \sqrt{1-k^2}.$$

Since the dn-periodic wave becomes the constant-amplitude wave of unit amplitude if $k = 0$, it is clear that the maximal instability rate is largest for the constant-amplitude wave with $k = 0$, monotonically decreasing in k, and vanishes for the soliton limit $k = 1$. As $k \to 1$, the horizontal band on **Figure 2** (right) shrinks to an eigenvalue at the origin.

For the cn-periodic wave **Eq. 2.12** with $u_1 = k$ and $u_2 = i\sqrt{1-k^2}$, the amplitude is k. Hence, we use the scaling transformation (2.3) with $\alpha = k^{-1}$ in order to normalize the amplitude to unity. Lax spectrum of the spectral problem **Eq. 3.2** for such an amplitude-normalized cn-periodic wave is shown on left panels of **Figure 3** for $k = 0.85$ (top) and $k = 0.95$ (bottom). The unstable spectrum on the Λ-plane is obtained from the same expressions $\Lambda = \pm 2i\sqrt{P(\lambda)}$ when λ traverses along the bands of the Lax spectrum outside $i\mathbb{R}$. The unstable spectrum resembles the figure-eight band as is shown on the right panels of **Figure 3**. The figure-eight band starts and ends at $\Omega = 0$ for $\lambda = \lambda_1$ and $\lambda = \lambda_2$. Stability spectrum for both examples is similar in spite of the differences in the Lax spectrum. The only difference is that the figure-eight band and the purely imaginary bands intersect for $k = 0.85$ (top) and do not intersect for $k = 0.95$ (bottom). Thus, the cn-periodic wave **Eq. 2.12** is spectrally and modulationally unstable. As $k \to 1$, the figure-eight band shrinks to an eigenvalue at the origin.

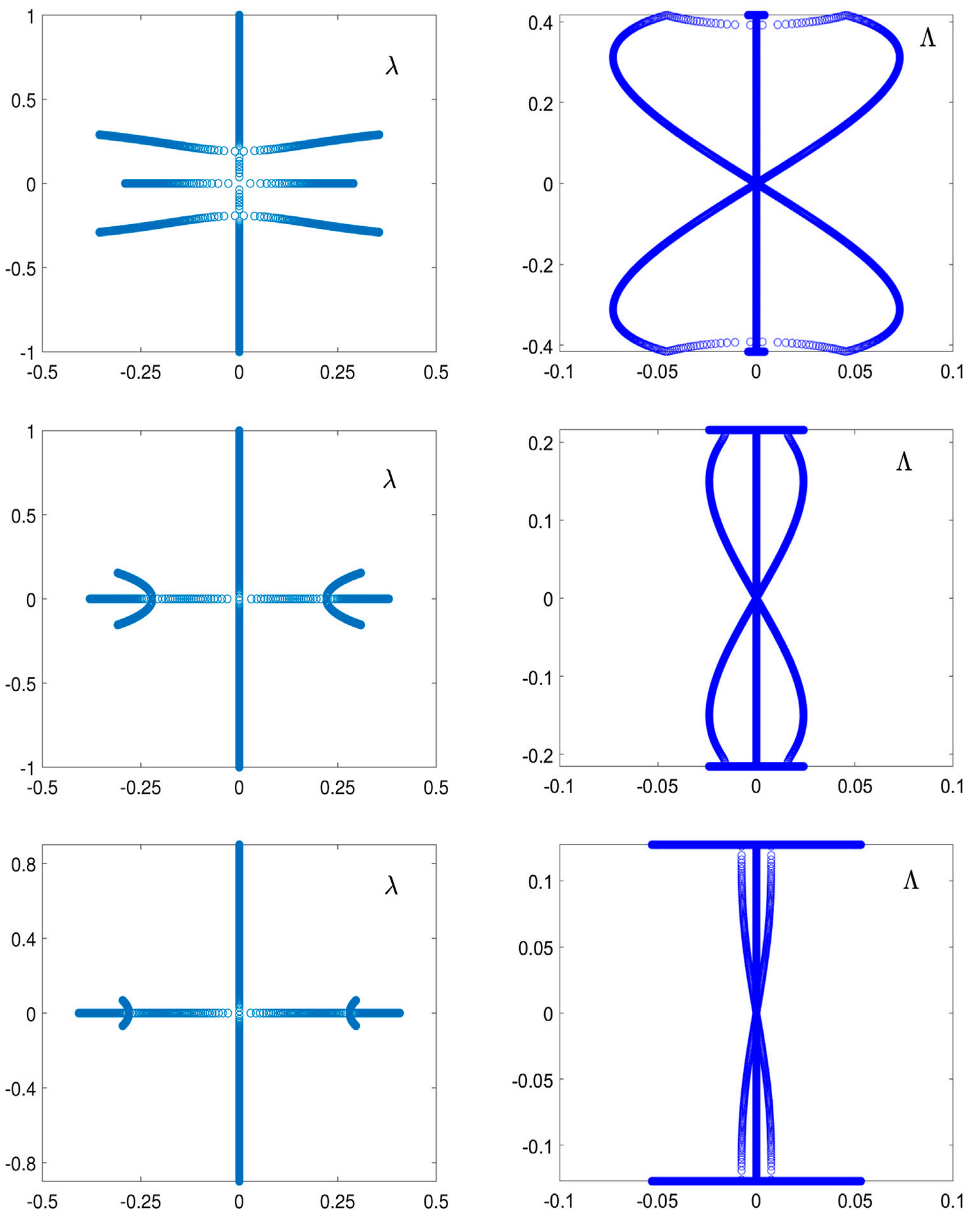

FIGURE 6 | The same as **Figure 5** but for the amplitude-normalized double-periodic wave (2.16) with $k = 0.3$ **(top)**, $k = 0.6$ **(middle)**, and $k = 0.9$ **(bottom)**.

Figure 4 compares the instability rates for different standing waves of the same unit amplitude. $\mathrm{Re}(\Lambda)$ is plotted versus the Floquet parameter θ in $\left[0, \frac{\pi}{L}\right]$ in **Eq. 3.4**. For the dn-periodic wave (left), we confirm that the growth rate is maximal for the constant-amplitude wave $(k = 0)$ and is monotonically decreasing as k is increased in $(0, 1)$. For the cn-periodic wave (right), the growth rate is also maximal in the limit $k \to 0$, for which the amplitude-normalized cn-periodic wave is expanded as

$$u(x) = \mathrm{cn}(k^{-1}x; k) \sim 0.5e^{ik^{-1}x} + 0.5e^{-ik^{-1}x} \quad \text{as} \quad k \to 0. \tag{3.17}$$

Due to the scaling transformation **Eq. 2.3** and the expansion **Eq. 3.17**, the maximal growth rate in the limit $k \to 0$ is 0.25 instead of 1 and the Floquet parameter θ, for which it is attained, diverges to infinity as $k \to 0$. As k increases in $(0, 1)$, the growth rate becomes smaller and the Floquet parameter θ for which $\mathrm{Re}(\Lambda) > 0$ moves toward the origin. The end point of the unstable band reaches $\theta = 0$, when the bands of the Lax spectrum outside $i\mathbb{R}$ do not intersect $i\mathbb{R}$ like on **Figure 3** (bottom).

4 INSTABILITY OF DOUBLE-PERIODIC WAVES

Here we describe the main result on how to compute the instability rates for the double-periodic waves by using the linear **Eqs. 2.5, 2.6**. We write the solutions **Eqs. 2.15, 2.16** in

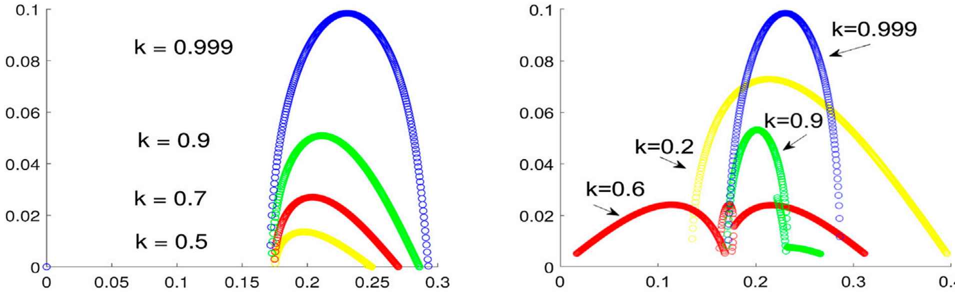

FIGURE 7 | Instability rate Re(Λ) versus the Floquet parameter θ for the amplitude-normalized double-periodic wave **Eq. 2.15 (left)** and the double-periodic wave **Eq. 2.16 (right)**. The values of k are given in the plots.

the form **Eq. 2.17**. We represent solution φ to the linear **Eqs. 2.5, 2.6** in the form:

$$\varphi_1(x,t) = \chi_1(x,t)e^{ibt+x\mu+t\Omega}, \quad \varphi_2(x,t) = \chi_2(x,t)e^{-ibt+x\mu+t\Omega}, \tag{4.1}$$

where $\mu, \Omega \in \mathbb{C}$ are spectral parameters and $\chi = (\chi_1, \chi_2)^T$ satisfies the following spectral problems:

$$\chi_x + \mu\chi = \begin{pmatrix} \lambda & \phi \\ -\bar{\phi} & -\lambda \end{pmatrix}\chi, \tag{4.2}$$

and

$$\chi_t + \Omega\chi = i\begin{pmatrix} \lambda^2 + \frac{1}{2}|\phi|^2 - b & \frac{1}{2}\frac{d\phi}{dx} + \lambda\phi \\ \frac{1}{2}\frac{d\bar{\phi}}{dx} - \lambda\bar{\phi} & -\lambda^2 - \frac{1}{2}|\phi|^2 + b \end{pmatrix}\chi. \tag{4.3}$$

Parameters $\mu, \Omega \in \mathbb{C}$ are independent of (x,t). This follows from the same compatibility of the linear Lax **Eqs. 2.5, 2.6** if $\psi(x,t)$ in **Eq. 2.17** satisfies the NLS **Eq. 2.1**.

By Floquet theorem, spectral parameters $\mu, \Omega \in \mathbb{C}$ are determined from the periodicity conditions $\chi(x+L,t) = \chi(x,t+T) = \chi(x,t)$ in terms of the spectral parameter λ. We distinguish between the space coordinate x and the time coordinate t in order to consider stability of the double-periodic waves **Eq. 2.17** in the time evolution of the NLS **Eq. 2.1**.

The Lax spectrum is defined by the condition that λ belongs to an admissible set for which the solution **Eq. 4.1** is bounded in x. Hence $\mu = i\theta$ with real θ in $\left[-\frac{\pi}{L}, \frac{\pi}{L}\right]$ and λ is computed from the spectral problem **Eq. 4.2** with $\chi(x+L,t) = \chi(x,t)$ for every $t \in \mathbb{R}$

With λ defined in the Lax spectrum, the spectral problem **Eq. 4.3** can be solved for the spectral parameter Ω under the condition that $\chi(x,t+T) = \chi(x,t)$ for every $x \in \mathbb{R}$. The corresponding solution to the linear system **Eqs. 4.2, 4.3** generates the solution $v(x,t)$ of the linearized system **Eq. 3.13** with $u \equiv \phi$ and $c = 0$ by means of the transformation formulas **Eqs. 3.14, 3.16**. Spectral parameter Ω is uniquely defined in the fundamental strip $\mathrm{Im}(\Omega) \in \left[-\frac{\pi}{T}, \frac{\pi}{T}\right]$, while $\mathrm{Re}(\Omega)$ determines the instability rate $\mathrm{Re}(\Lambda)$ by $\Lambda = 2\Omega$.

If $\mathrm{Re}(\Lambda) > 0$ for λ in the Lax spectrum, the double-periodic wave (2.17) is called *spectrally unstable*. The amplitude-normalized double-periodic waves are taken by using the scaling transformation (2.3). We observe again that the unstable spectrum with $\mathrm{Re}(\Lambda) > 0$ is related with λ in the Lax spectrum outside the imaginary axis.

For the amplitude-normalized double-periodic wave **Eq. 2.15** with $k = 0.85$ (top) and $k = 0.95$ (bottom), **Figure 5** shows the Lax spectrum of the spectral problem **Eq. 4.2** with $\mu = i\theta$ and $\theta \in \left[-\frac{\pi}{L}, \frac{\pi}{L}\right]$ on the λ-plane (left) and the stability spectrum on the Λ-plane (right). The unstable spectrum is located at the boundary $\mathrm{Im}(\Lambda) = \pm\frac{2\pi}{T}$ of the strip for every $k \in (0,1)$. The double-periodic wave **Eq. 2.15** is spectrally unstable.

Figure 6 shows the same as **Figure 5** but for the amplitude-normalized double-periodic wave **Eq. 2.16** with $k = 0.3$ (top), $k = 0.6$ (middle), and $k = 0.9$ (bottom). The Lax spectrum on the λ-plane has three bands, two of which are connected either across the imaginary axis (top) or across the real axis (middle and bottom), the third band is located on the real axis. The unstable spectrum on the Λ-plane includes the figure-eight band and bands located near the boundary $\mathrm{Im}(\Lambda) = \pm\frac{2\pi}{T}$. As $k \to 1$, the figure-eight band becomes very thin and the stability spectrum looks similar to the one on **Figure 5** because both the double-periodic solutions approach the Akhmediev breather **Eq. 2.18**.

Figure 7 compares the instability rates for different double-periodic waves of the same unit amplitude. $\mathrm{Re}(\Lambda)$ is plotted versus the Floquet parameter θ in $\left[0, \frac{\pi}{L}\right]$, where $\mu = i\theta$ is defined in **Eq. 4.2**.

For the amplitude-normalized double-periodic wave **Eq. 2.15** (left), the instability rate is maximal as $k \to 1$, that is, at the Akhmediev breather **Eq. 2.18**. The unstable band starts with the same cut-off value of θ and extends all the way to $\theta = \frac{\pi}{L}$. When $k \to 0$, the instability rates quickly decrease as the double-periodic wave approaches the NLS soliton **Eq. 2.19**.

For the amplitude-normalized double-periodic wave **Eq. 2.16** (right), the instability rate is large in the limit $k \to 0$, when the double-periodic wave is close to the particular cn-periodic wave **Eq. 2.20**. Then, the rates decrease when k is increased, however, the rates increase again and reach the maximal values as $k \to 1$ when the double-periodic wave approaches the Akhmediev breather **Eq. 2.18**.

5 CONCLUSION

We have computed the instability rates for the double-periodic waves of the NLS equation. By using the Lax pair of linear equations, we obtain the Lax spectrum with the Floquet theory in the spatial coordinate at fixed t and the stability spectrum with the Floquet theory in the temporal coordinate at fixed x. This separation of variables is computationally simpler than solving the full two-dimensional system of linearized NLS equations on the double-periodic solutions.

As the main outcome of the method, we have shown instability of the double-periodic solutions and have computed their instability rates, which are generally smaller compared to those for the standing periodic waves.

The concept can be extended to other double-periodic solutions of the NLS equation which satisfy the higher-order Lax–Novikov equations. Unfortunately, the other double-periodic solutions are only available in Riemann theta functions of genus $d \geq 2$, and for practical computations, one needs to construct such double-periodic solutions numerically, similarly to what was done in [41]. This task is opened for further work.

AUTHOR CONTRIBUTIONS

The author confirms being the sole contributor of this work and has approved it for publication.

ACKNOWLEDGMENTS

This work was supported in part by the National Natural Science Foundation of China (No. 11971103).

REFERENCES

1. Peregrine DH. Water waves, nonlinear Schrödinger equations and their solutions. *J Aust Math Soc Series B Appl Math* (1983) 25:16–43. doi:10.1017/s0334270000003891
2. Akhmediev NN, Eleonsky VM, Kulagin NE. Generation of periodic trains of picosecond pulses in an optical fiber: exact solutions. *Sov Phys JETP* (1985) 62: 894–899.
3. Gelash AA, “Formation of rogue waves from a locally perturbed condensate”, *Phys Rev E* (2018) 97:022208. doi:10.1103/PhysRevE.97.022208
4. Zakharov VE, Gelash AA, “Nonlinear stage of modulation instability”, *Phys Rev Lett* (2013) 111:054101. doi:10.1103/PhysRevLett.111.054101
5. Gelash AA, Agafontsev DS, “Strongly interacting soliton gas and formation of rogue waves”, *Phys Rev E* (2018) 98:042210. doi:10.1103/physreve.98.042210
6. Gelash AA, Agafontsev D, Zakharov V, El G, Randoux S, Suret P, “Bound state soliton gas dynamics underling the spontaneous modulational instability”, *Phys Rev Lett* (2019) 123:234102. doi:10.1103/physrevlett.123.234102
7. Agafontsev DS, Zakharov VE. Integrable turbulence and formation of rogue waves. *Nonlinearity* (2015) 28:2791–2821. doi:10.1088/0951-7715/28/8/2791
8. Agafontsev DS, Zakharov VE. Integrable turbulence generated from modulational instability of conoidal waves. *Nonlinearity* (2016) 29: 3551–3578. doi:10.1088/0951-7715/29/11/3551
9. Randoux S, Suret P, Chabchoub A, Kibler B, El G, “Nonlinear spectral analysis of Peregrine solitons observed in optics and in hydrodynamic experiments”, *Phys Rev E* (2018) 98:022219. doi:10.1103/PhysRevE.98.022219
10. Dudley JM, Genty G, Mussot A, Chabchoub A, Dias F. Rogue waves and analogies in optics and oceanography. *Nat Rev Phys* (2019) 1:675. doi:10.1038/s42254-019-0100-0
11. Copie F, Randoux S, Suret P, “The Physics of the one-dimensional nonlinear Schrödinger equation in fiber optics: rogue waves, modulation instability and self-focusing phenomena”, *Reviews in Physics* (2020) 5:100037. doi:10.1016/j.revip.2019.100037
12. Biondini G, Mantzavinos D, “Universal nature of the nonlinear stage of modulational instability”, *Phys Rev Lett* (2016) 116:043902. doi:10.1103/PhysRevLett.116.043902
13. Biondini G, Li S, Mantzavinos D, Trillo S. Universal behavior of modulationally unstable media. *SIAM Rev* (2018) 60:888–908. doi:10.1137/17m1112765
14. Grinevich PG, Santini PM. The finite gap method and the analytic description of the exact rogue wave recurrence in the periodic NLS Cauchy problem. 1. *Nonlinearity* (2018) 31:5258–5308. doi:10.1088/1361-6544/aaddcf
15. Grinevich PG, Santini PM. The finite-gap method and the periodic NLS Cauchy problem of anomalous waves for a finite number of unstable modes. *Russ Math Surv* (2019) 74:211–263. doi:10.1070/rm9863
16. Bilman D, Ling L, Miller PD. Extreme superposition: rogue waves of infinite order and the Painlevé-III hierarchy. *Duke Math J* (2020) 169:671–760. doi:10.1215/00127094-2019-0066
17. Bilman D, Miller PD. A robust inverse scattering transform for the focusing nonlinear schrödinger equation. *Commun Pure Appl Math* (2019) 72: 1722–1805. doi:10.1002/cpa.21819
18. Slunyaev AV, Pelinovsky EN, “Role of multiple soliton Interactions in the generation of rogue waves: the modified Korteweg-de Vries framework”, *Phys Rev Lett* (2016) 117:214501. doi:10.1103/PhysRevLett.117.214501
19. Bilman D, Buckingham R. Large-order asymptotics for multiple-Pole solitons of the focusing nonlinear schrödinger equation. *J Nonlinear Sci* (2019) 29: 2185–2229. doi:10.1007/s00332-019-09542-7
20. Chen J, Pelinovsky DE, “Rogue periodic waves of the focusing nonlinear Schrödinger equation”, *Proc R Soc A* (2018) 474:20170814. doi:10.1098/rspa.2017.0814
21. Kedziora DJ, Ankiewicz A, Akhmediev N. Rogue waves and solitons on a conoidal background. *Eur Phys J Spec Top* (2014) 223:43–62. doi:10.1140/epjst/e2014-02083-4
22. Feng BF, Ling L, Takahashi DA. Multi-breather and high-order rogue waves for the nonlinear Schrödinger equation on the elliptic function background. *Stud Appl Math* (2020) 144:46–101. doi:10.1111/sapm.12287
23. Chen J, Pelinovsky DE, White RE, “Periodic standing waves in the focusing nonlinear Schrödinger equation: rogue waves and modulation instability”, *Physica D* (2020) 405:132378. doi:10.1016/j.physd.2020.132378
24. Bronski JC, Hur VM, Johnson MA. “Instability in equations of KdV type”, In: *New approaches to nonlinear waves, lecture notes in phys*. Cham: Springer (2016) 908:83–133.
25. Kamchatnov AM. On improving the effectiveness of periodic solutions of the NLS and DNLS equations. *J Phys Math Gen* (1990) 23:2945–2960. doi:10.1088/0305-4470/23/13/031
26. Kamchatnov A. New approach to periodic solutions of integrable equations and nonlinear theory of modulational instability. *Phys Rep* (1997) 286: 199–270. doi:10.1016/s0370-1573(96)00049-x
27. Deconinck B, Segal BL. The stability spectrum for elliptic solutions to the focusing NLS equation. *Physica D* (2017) 346:1–19. doi:10.1016/j.physd.2017.01.004
28. Deconinck B, Upsal J. The orbital stability of elliptic solutions of the focusing nonlinear schrödinger equation. *SIAM J Math Anal* (2020) 52:1–41. doi:10.1137/19m1240757
29. Upsal J, Deconinck B. Real Lax spectrum implies spectral stability. *Stud Appl Math* (2020) 145:765–790. doi:10.1111/sapm.12335
30. Xu G, Chabchoub A, Pelinovsky DE, Kibler B, “Observation of modulation instability and rogue breathers on stationary periodic waves”, *Phys Rev Res* (2020) 2:033528. doi:10.1103/physrevresearch.2.033528
31. Akhmediev NN, Eleonskii VM, Kulagin NE. Exact first-order solutions of the nonlinear Schrödinger equation. *Theor Math Phys* (1987) 72:809–818. doi:10.1007/bf01017105

32. Akhmediev N, Ankiewicz A, Soto-Crespo JM, "Rogue waves and rational solutions of the nonlinear Schrödinger equation", *Phys Rev E Stat Nonlinear Soft Matter Phys* (2009) 80:026601. doi:10.1103/PhysRevE.80.026601
33. Kimmoun O, Hsu HC, Branger H, Li MS, Chen YY, Kharif C, et al. Modulation instability and phase-shifted Fermi-pasta-ulam recurrence, *Sci Rep* (2016) 6: 28516. doi:10.1038/srep28516
34. Chen J, Pelinovsky DE, White RE, "Rogue waves on the double-periodic background in the focusing nonlinear Schrödinger equation", *Phys Rev E* (2019) 100:052219. doi:10.1103/PhysRevE.100.052219
35. Calini A, Schober CM. Characterizing JONSWAP rogue waves and their statistics via inverse spectral data. *Wave Motion* (2017) 71:5–17. doi:10.1016/j.wavemoti.2016.06.007
36. Conforti M, Mussot A, Kudlinski A, Trillo S, Akhmediev N, "Doubly periodic solutions of the focusing nonlinear Schrödinger equation: recurrence, period doubling, and amplification outside the conventional modulation-instability band", *Phys Rev A* (2020) 101:023843. doi:10.1103/physreva.101.023843
37. Vanderhaegen G, Szriftgiser P, Naveau C, Kudlinski A, Conforti M, Trillo S, et al. Observation of doubly periodic solutions of the nonlinear Schrödinger equation in optical fibers. *Opt Lett* (2020) 45:3757–3760. doi:10.1364/OL.394604
38. Smirnov AO. Solution of a nonlinear Schrödinger equation in the form of two-phase freak waves. *Theor Math Phys* (2012) 173:1403–1416. doi:10.1007/s11232-012-0122-6
39. Smirnov AO. Periodic two-phase "Rogue waves". *Math Notes* (2013) 94: 897–907. doi:10.1134/s0001434613110266
40. Wright OC. Effective integration of ultra-elliptic solutions of the focusing nonlinear Schrödinger equation. *Phys Nonlinear Phenom* (2016) 321-322: 16–38. doi:10.1016/j.physd.2016.03.002
41. Bertola M, El GA, Tovbis A, "Rogue waves in multiphase solutions of the focusing nonlinear Schrödinger equation", *Proc R Soc A* (2016) 472:20160340. doi:10.1098/rspa.2016.0340
42. Bertola M, Tovbis A. Maximal amplitudes of finite-gap solutions for the focusing Nonlinear Schrödinger equation. *Commun Math Phys* (2017) 354: 525–47. doi:10.1007/s00220-017-2895-9
43. Wright OC. Sharp upper bound for amplitudes of hyperelliptic solutions of the focusing nonlinear Schrödinger equation. *Nonlinearity* (2019) 32:1929–1966. doi:10.1088/1361-6544/aafbd2
44. Sulem C, Sulem PL, The nonlinear Schrödinger equation: self-focusing and wave collapse. In: *Applied mathematical sciences*. New York: Springer-Verlag (1999) 139.
45. Fibich G, The nonlinear Schrödinger equation: singular solutions and optical collapse. In: *Applied mathematical sciences*. New York: Springer-Verlag (2015) 192.
46. Pelinovsky DE, White RE, "Localized structures on librational and rotational travelling waves in the sine-Gordon equation", *Proc R Soc A* (2020) 476: 20200490. doi:10.1098/rspa.2020.0490

Conflict of Interest: The author declares that the research was conducted in the absence of any commercial or financial relationships that could be construed as a potential conflict of interest.